JOURNAL OF THE ROYAL SOCIETY Interface

J. R. Soc. Interface (2010) **7**, 1641–1645
doi:10.1098/rsif.2010.0036
Published online 3 March 2010

REPORT

A novel route for processing cobalt–chromium–molybdenum orthopaedic alloys

Bhairav Patel[1], Fawad Inam[2], Mike Reece[2], Mohan Edirisinghe[1,*], William Bonfield[1,3], Jie Huang[1] and Arash Angadji[4]

[1]*Department of Mechanical Engineering, University College London, Torrington Place, London WC1E 7JE, UK*
[2]*School of Engineering and Materials Science and Nanoforce Technology, Queen Mary University of London, London E1 4NS, UK*
[3]*Department of Materials Science and Metallurgy, University of Cambridge, Pembroke Street, Cambridge CB2 3QZ, UK*
[4]*Furlong Research Charitable Foundation, Furlong House, 10a Chandos Street, London W1G 9DQ, UK*

Spark plasma sintering has been used for the first time to prepare the ASTM F75 cobalt–chromium–molybdenum (Co–Cr–Mo) orthopaedic alloy composition using nanopowders. In the preliminary work presented in this report, the effect of processing variables on the structural features of the alloy (phases present, grain size and microstructure) has been investigated. Specimens of greater than 99.5 per cent theoretical density were obtained. Carbide phases were not detected in the microstructure but oxides were present. However, harder materials with finer grains were produced, compared with the commonly used cast/wrought processing methods, probably because of the presence of oxides in the microstructure.

Keywords: processing; biomedical; metallic; orthopaedics

1. INTRODUCTION

Millions of people suffer from bone and joint inflammatory problems. These diseases usually result in surgery of the affected area and in extreme cases total joint replacements are required. The most common type of joint replacements are of the hip and knee joints. There has been a revived interest in metal-on-metal (MoM) hip replacements over the past 20 years (Dumbleton & Manley 2005). Various metallic alloys have been successfully used for joint replacement (Davis 2003), but three metals and their alloys, which are stainless steel, titanium and cobalt (Co)-based alloys, have been predominantly used for joint replacement.

Co-based alloys are widely implanted, both as surface replacements and for total hip replacements (Morral 1966; Scales 1971). Compared with other materials, Co alloys have a higher wear resistance (Sieber *et al.* 1999); therefore, less wear debris can form and there is less risk of loosening or failure of the implant. These alloys are also favourable because of their superior mechanical properties, most significantly fatigue strength and hardness, and corrosion resistance owing to the chromium (Cr), which forms a protective oxide layer upon the surface. The most common Co-based alloy used in clinical application is the Co–Cr–Mo system, which consists of 28 wt% Cr, 6 wt% Mo, and balance wt% of Co (ASTM Standard F75 1998), which is extensively used in femoral and acetabular components (Unsworth 1981). A typical microstructure of this as-cast Co–Cr–Mo alloy consists of a solid Co matrix with fine carbides, which are Cr- and Mo-rich particles, distributed in the microstructure (ASTM Standard F75 1998). The presence of carbides, due to the melt processing, can be a problem, as, if these carbide particles are dislodged, accelerated localized wear can result.

There are two conventional methods to fabricate the alloy—either as cast or wrought. The former simply requires the implant to be cast into shape, and is usually used for complex shapes such as the stem (Hansen 2008). The latter method requires the cast ingot to be plastically deformed into the desired shape and subsequently machined, and is usually used for simpler shapes such as a femoral head (Hansen 2008). Another point of view is that wrought alloys are better than cast material because of their superior mechanical properties (Süry & Semlitsch 1978). The forging process can be either hot or cold and promotes plastic deformation (Immarigeon *et al.* 1984). Powder processing is an alternative method of fabricating this alloy and has been shown to produce significant improvements (Bardos 1979; Kilner *et al.* 1986; Dewidar *et al.* 2006) as this route generates a structure with finer grains, which relates to the enhancement in the properties, especially strength, toughness and ductility (Brown 2001).

One of the key stages of powder processing is sintering of the powder to fuse the particles together. A superior but simple sintering processing is spark plasma sintering (SPS), which produces highly dense materials with minimum grain growth. This is achieved by a pulsed electrical current heating the material while applying a pressure to compact the powdered material (Shen *et al.* 2003; Yan *et al.* 2005). This process has the ability to densify nanopowders, in order to produce microstructures with finer grains and superior mechanical properties (Johnson 1991; Gao *et al.* 1999). It has been used to produce various metallic alloys, ceramics and composites for functional and structural uses (Yoritoshi *et al.* 2005; Munir *et al.* 2006; Inam *et al.* 2008; Dusza *et al.* 2009). In this report we use nanopowders of Co, Cr and Mo to powder process Co–Cr–Mo alloy with overall composition equal to the F75

*Author for correspondence (m.edirisinghe@ucl.ac.uk).

Received 25 January 2010
Accepted 9 February 2010

Table 1. The average particle size of the as-supplied powder. In the case of Cr, scanning electron micrograph showed the particles to be coarser but this may be because of agglomerates.

powder	Co	Cr	Mo
average particle size (nm)	28	100	85
product number	CO-M-O2-NP	CR-M-O2-NP	MO-M-O2-NP

Table 2. Details of ball-milled SPS sample processing conditions, grain size and hardness.

sintering temperature (°C)	dwell time (min)	pressure (MPa)	melting	average grain size (μm)	average hardness (Vickers)
1050	10	75	no	1.3	742
1050	10	100	no	1.2	754
1075	10	100	no	1.4	797
1100	10	75	slight	1.0	707
1150	3	75	yes	0.6	684
1175	3	75	yes	0.6	683

composition, using SPS. The resulting microstructures are analysed and related to the processing.

2. EXPERIMENTAL DETAILS

2.1. Materials

Elemental powders of Co, Cr and Mo (American Elements, USA) were used and their typical particle sizes are given in table 1.

2.2. Mixing method

Fifty grams of the Co–Cr–Mo powder was measured in the 66 : 28 : 6 wt% ratio, respectively, and added to a nylon ball-milling pot containing zirconia balls. A process control agent (PCA; 120 ml ethanol) was added to the milling pot and the mixture was milled for 72 h. The PCA reduces oxidation and breaks up any agglomerates that may have been formed. The milled mixture was removed into a stainless steel pan and heated to 80°C for 24 h to evaporate the ethanol, leaving a dry powder. A 250 μm sieve was used to remove any agglomerates.

2.3. Spark plasma sintering

SPS was performed using a HPD25/1 (FCT Systeme, Germany) furnace under vacuum (5 Pa). Batches containing 3.5 g of mixed powder were loaded into the 20 mm diameter cylindrical graphite die. The heating rate was set at 50°C min^{-1} and the cooling rate at 130°C min^{-1}. Table 2 shows the sintering conditions that were adopted for each sample.

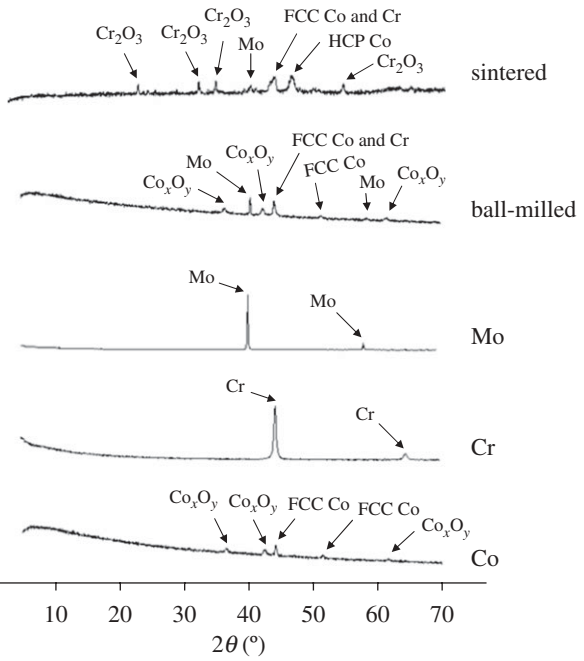

Figure 1. XRD results of the as-received, ball-milled and sintered powders.

2.4. Characterization

The three elemental powders and ball-milled powder were analysed for their phase content using an X'PERT PRO Philips diffractometer operating with CuKα radiation at 45 kV and 40 mA in the scanning range of 30–90° with a step size of 0.03° and a scan time of 400 s per datum point.

The densities of the sintered samples were studied using field emission scanning electron microscopy (FE-SEM; FEI Inspect F, 10 kV, working distance 10 mm) images of the surface after thresholding the porosity using UTHSCSA ImageTool 3.0 software. Samples of sintered compact were also mounted in epoxy resin. Once set, the surface was polished using 1200P–4000P SiC grading paper. The polished samples were studied for their microstructure, including grain size, using field emission scanning electron microscopy. To etch the grains, the samples were dipped in an etching solution of 25 ml ethanol, 5 ml 1.0 M HCl and 1 g of $CuCl_2$ for 10 s and rinsed out with acetone to remove any excess etchant (Tang *et al.* 2008). Element-mapping of elements was carried out using an integrated X-ray energy-dispersive attachment (EDS) with an EDAX UTW detector. The compacts were also studied using an X'PERT PRO Philips diffractometer operating with CuKα radiation at 45 kV and 40 mA in the scanning range of 5–70° with a step size of 0.03° and a scan time of 400 s per datum point. The microhardness of the compacts was measured using a Leco M-400-G hardness tester and the Vickers indentation method (ASTM Standard E92 2003).

3. RESULTS AND DISCUSSION

The powders show the peaks of all the element phases (figure 1). In the case of Co, oxide peaks are also

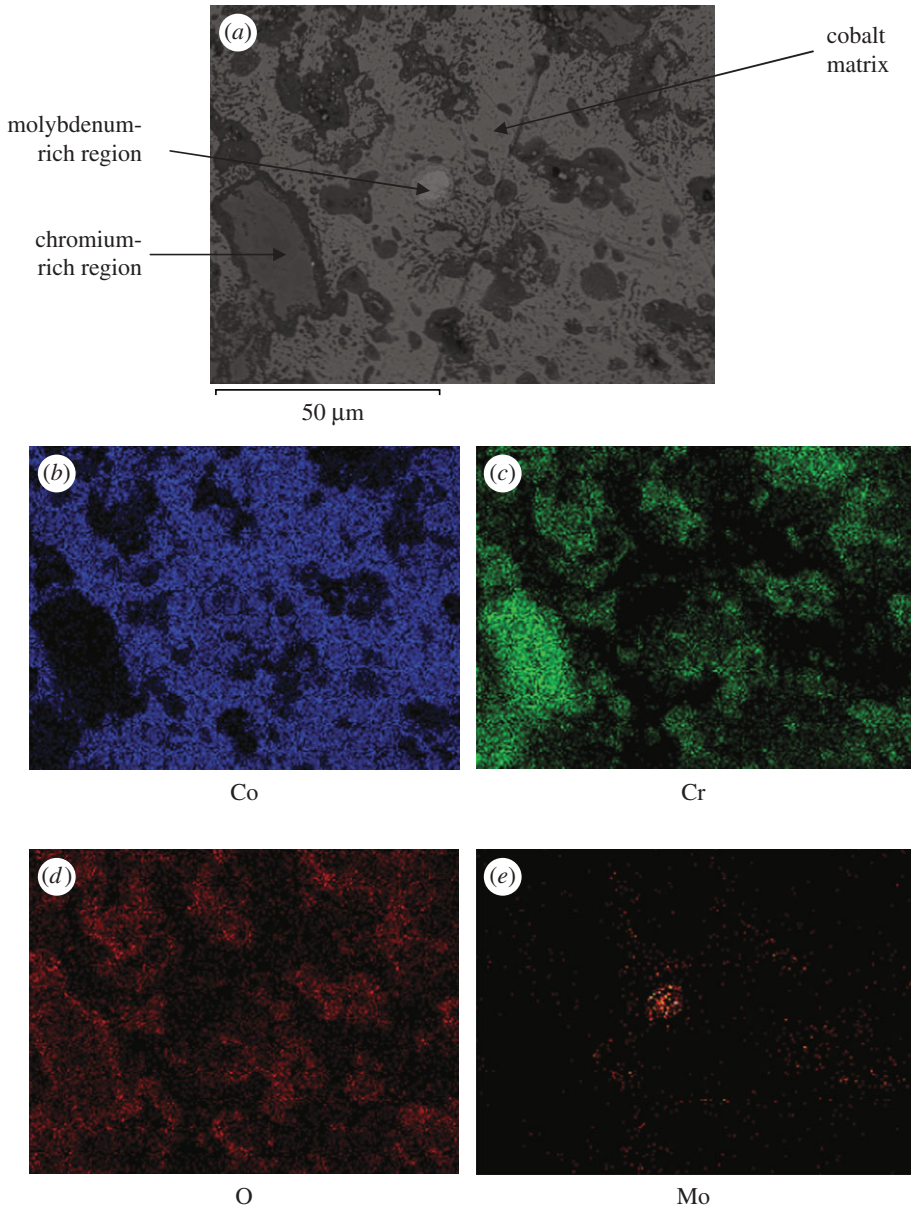

Figure 2. (*a*) Typical microstructure prepared by ball-milling compact and SPS to 1075°C with (*b*) Co, (*c*) Cr, (*d*) O and (*e*) Mo distribution highlighted.

identified; this is probably because of surface coatings on the powder in order to reduce its oxidation and enable safe handling. Ball milling the powders did not result in any significant contamination (figure 1). SPS has resulted in the formation of new phases in the bulk material and these are identified in figure 1.

The microstructure of the SPS compacts is different from that of typical cast or wrought alloys. The conventional methods form a Co matrix with carbides distributed randomly (ASTM Standard F75 1998), but the SPS microstructure (figure 2) consists of a Co matrix with Cr- and Mo-rich regions. Also, from figures 1 and 2, it is clear that the Cr in association with O forms Cr_2O_3 in the microstructure. The necessary O could have come from two sources: from Co or from the atmosphere during mixing. Also, the hexagonal close-packed (HCP) Co structure has been formed because of the martensitic transformation (Montero-Ocampo *et al.* 2002). No carbides are present in the microstructure, which corresponds well with the XRD peaks identified in figure 1.

All ball-milled sintered compacts were near-full density (>99.5%). Above 1075°C, melting occurred, whereby small droplets appeared at the rim of the die after sintering, which reduced the relative density to 98%. During SPS, the powder particles are heated by discharge action from the electrical current and, because of the high pressures and rapid cooling, the molten mix is forced outward, forming droplets (Tang *et al.* 2008).

Compared with the conventional processing methods, which produce samples with a grain size of approximately 7 µm (Salinas-Rodriguez & Rodriguez-Galicia 1996), the SPS compacts originating from nanopowders have a much finer grain structure, as indicated in table 2, and this is beneficial for achieving high strength and high toughness products. The use of

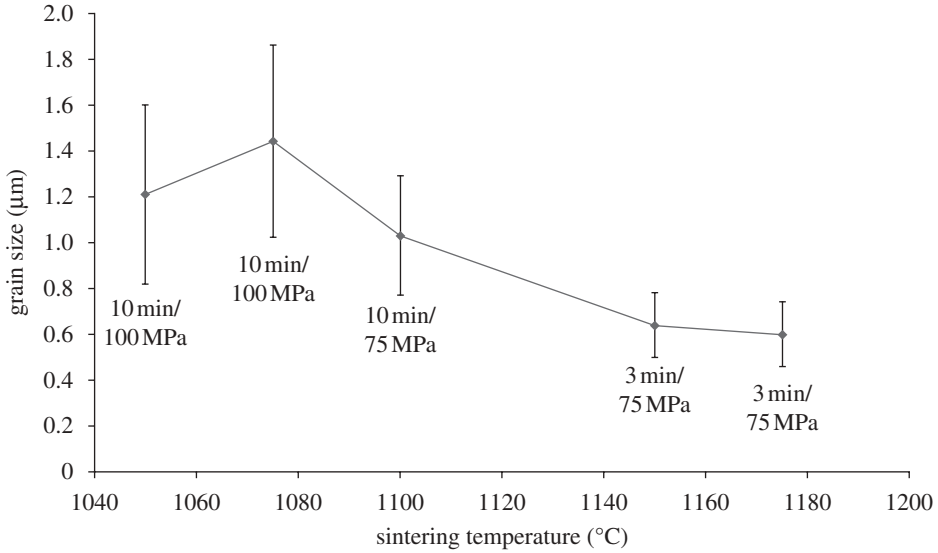

Figure 3. Variation of grain size as a function of sintering temperature.

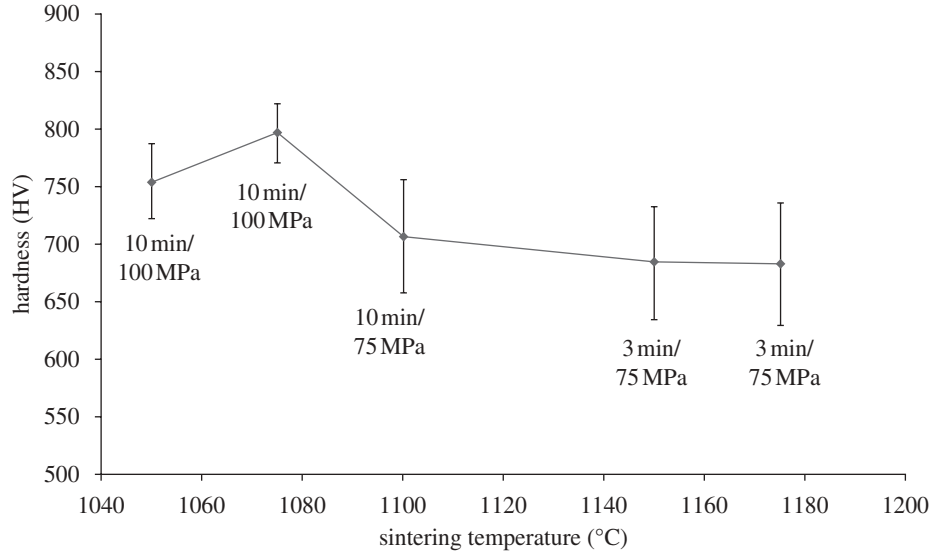

Figure 4. Variation of hardness as a function of sintering temperature.

rapid heating and cooling in SPS limits the increase in grain size because of increasing temperature (figure 3), and above 1075°C melting and resolidification is accompanied by an even slightly lower grain size.

The variation of hardness and grain size as a function of sintering temperature shows similar profiles (figures 3 and 4). Compared with the conventional routes of forming similar materials, which result in a hardness of 300–480 Vickers (Devine & Wulff 1975), the SPS compacts are much harder, as indicated in table 2. The increase in the sintering temperature increases the average hardness of the compact initially (figure 4). However, above 1075°C the hardness decreases, probably because of the melting observed (table 2). The maximum average hardness achieved was 797 Vickers, and this must be owing to a combination of factors such as fine grains and the distribution of the oxides in the microstructure, which will be studied by transmission electron microscopy.

4. CONCLUSIONS

This preliminary work shows that the F75 orthopaedic alloy composition free of carbide phases can be made via SPS powder processing and this is a vital breakthrough. The compacts produced are near-full density and contain fine grains. They are of higher hardness than cast or wrought products despite the absence of carbides in the microstructure. The gain in hardness is because of the presence of oxides in the microstructure and we hope to quantify the oxide content in the future. Therefore, the SPS route offers significant advantages over the conventional cast and wrought routes used to prepare this alloy for orthopaedic applications.

The next step is to evaluate the tribological performance (wear, friction, lubrication regimes) of this SPS-processed material and compare its performance with conventional MoM products (cast and wrought).

This work is supported by the Furlong Research Charitable Foundation.

REFERENCES

ASTM Standard E92 2003 Standard test method for Vickers hardness of metallic materials. West Conshohocken, PA: ASTM International. www.astm.org. (doi:10.1520/E0092-82R03)

ASTM Standard F75 1998 Standard specification for cast cobalt–chromium–molybdenum alloy for surgical implant applications. West Conshohocken, PA: ASTM International. www.astm.org. (doi:10.1520/F0075-07)

Bardos, D. I. 1979 High strength Co–Cr–Mo alloy by hot isostatic pressing of powder. *Biomater. Med. Devices Artif. Organs* **7**, 73–80. (doi:10.3109/10731197909119373)

Brown, R. 2001 Powder metallurgical processing improves high-carbon Co–Cr–Mo alloy for orthopaedic implants. *Cobalt News* **1/4**, 9–14.

Davis, J. R. 2003 *Handbook of materials for medical devices*, ch. 1. Materials Park, OH: ASM International.

Devine, T. M. & Wulff, A. 1975 Cast vs. wrought cobalt-chromium surgical implant alloys. *J. Biomed. Mater. Res.* **9**, 151–167. (doi:10.1002/jbm.820090205)

Dewidar, M. M., Yoon, H.-C. & Lim, J. K. 2006 Mechanical properties of metals for biomedical applications using powder metallurgy process: a review. *Met. Mater. Int.* **12**, 193–206. (doi:10.1007/bf03027531)

Dumbleton, J. H. & Manley, M. T. 2005 Metal-on-metal total hip replacement: what does the literature say? *J. Arthoplasty* **20**, 174–188. (doi:10.1016/j.arth.2004.08.011)

Dusza, J., Blugan, G., Morgiel, J., Kuebler, J., Inam, F., Peijs, T., Reece, M. J. & Puchy, V. 2009 Hot pressed and spark plasma sintered zirconia/carbon nanofibre composites. *J. Eur. Ceram. Soc.* **29**, 3177–3184. (doi:10.1016/j.jeurceramsoc.2009.05.030)

Gao, L., Wang, H. Z., Hong, J. S., Miyamoto, H., Miyamoto, K., Nishikawa, Y. & Torre, S. D. D. L. 1999 SiC-ZrO_2(3Y)-Al_2O_3 nanocomposites superfast densified by spark plasma sintering. *Nanostruct. Mater.* **11**, 43–49. (doi:10.1016/S0965-9773(98)00160-3)

Hansen, D. C. 2008 Metal corrosion in the human body: the ultimate bio-corrosion scenario. *Electrochem. Soc. Interface* **17**, 31–34.

Immarigeon, J. P., Rajan, K. & Wallace, W. 1984 Microstructural changes during isothermal forging of a Co–Cr–Mo alloy. *Metall. Mater. Trans. A* **15**, 339–345. (doi:10.1007/bf02645120)

Inam, F., Yan, H., Reece, M. J. & Peijs, T. 2008 Dimethylformamide: an effective dispersant for making ceramic–carbon nanotube composites. *Nanotechnology* **19**, 1–5. (doi:10.1088/0957-4484/19/19/195710)

Johnson, D. L. 1991 Microwave and plasma sintering of ceramics. *Ceram. Int.* **17**, 295–300. (doi:10.1016/0272-8842(91)90025-u)

Kilner, T., Laanemäe, W. M., Pilliar, R., Weatherly, G. C. & MacEwen, S. R. 1986 Static mechanical properties of cast and sinter-annealed cobalt-chromium surgical implants. *J. Mater. Sci.* **21**, 1349–1356. (doi:10.1007/BF00553274)

Montero-Ocampo, C., Juarez, R. & Salinas-Rodriguez, A. 2002 Effect of FCC-HCP phase transformation produced by isothermal aging on the corrosion resistance of a Co-27Cr-5Mo-0.05C alloy. *Metall. Mater. Trans. A* **33**, 2229–2235. (doi:10.1007/s11661-002-0054-0)

Morral, F. R. 1966 Cobalt alloys as implants in humans. *J. Mater.* **1**, 384–412.

Munir, Z. A., Anselmi-Tamburini, U. & Ohyanagi, M. 2006 The effect of electric field and pressure on the synthesis and consolidification of materials: a review of the spark plasma sintering method. *J. Mater. Sci.* **41**, 763–777. (doi:10.1007/s10853-006-6555-2)

Salinas-Rodriguez, A. & Rodriguez-Galicia, J. L. 1996 Deformation behavior of low-carbon Co–Cr–Mo alloys for low-friction implant applications. *J. Biomed. Mater. Res.* **31**, 409–419. (doi:10.1002/(SICI)1097-4636(199607)31:3<409::AID-JBM16>3.0.CO;2-D)

Scales, J. T. 1971 Examination of implants removed from patients. *J. Bone Joint Surg.* [*Br*] **53B**, 344–346.

Shen, Z., Peng, H. & Nygren, M. 2003 Formidable increase in the superplasticity of ceramics in the presence of an electric field. *Adv. Mater.* **15**, 1006–1009. (doi:10.1002/adma.200304863)

Sieber, H. P., Rieker, C. B. & Köttig, P. 1999 Analysis of 118 second generation metal-on-metal retrieved hip implants. *J. Bone Joint Surg.* [*Br*] **81**, 46–50. (doi:10.1302/0301-620X.81B1.9047)

Süry, P. & Semlitsch, M. 1978 Corrosion behaviour of cast and forged cobalt based alloys for double-alloy joint endoprostheses. *J. Biomed. Mater. Res.* **12**, 723–741. (doi:10.1002/jbm.820120512)

Tang, C. F., Pan, F., Qu, X. H., Jia, C. C., Duan, B. H. & He, X. B. 2008 Spark plasma sintering cobalt base superalloy strengthened by Y–Cr–O compound through high-energy spark plasma sintering cobalt base superalloy strengthened by Y–Cr–O compound through high-energy milling. *J. Mater. Process. Technol.* **204**, 111–116. (doi:10.1016/j.jmatprotec.2007.10.084)

Unsworth, A. 1981 Artificial joints. In *An introduction to the bio-mechanics of joints and joint replacement* (eds D. Dowson & V. Wright), pp. 134–139. London, UK: Mechanical Engineering Publications.

Yan, H., Zhang, H., Ubic, R., Reece, M. J., Liu, J., Shen, Z. & Zhang, Z. 2005 A lead-free high-curie-point ferroelectric ceramic, $CaBi_2Nb_2O_9$. *Adv. Mater.* **17**, 1261–1265. (doi:10.1002/adma.200401860)

Yoritoshi, M., Yuichiro, K., Nobuhiro, T., Naoko, H., Kiyoshi, M. & Yoshihiru, O. 2005 Microstructures and mechanical properties of bulk nanocrystalline Fe–Al–C alloys made by mechanically alloying with subsequent spark plasma sintering. *Sci. Technol. Adv. Mater.* **5**, 133–143. (doi:10.1016/j.stam.2003.11.004)